Health monitoring in composite structures using piezoceramic sensors and fiber optic sensors

C. G. Kim[1], D. U. Sung[2], D. H. Kim[1], H. J. Bang[1].

1. *Division of Aerospace Engineering, KAIST, Daejeon, Korea*
2. *Functional System Test Team II, R&D Division, Hyundai Motor Co.*

Abstract: Health monitoring is a major concern not only in the design and manufacturing but also in service stages for composite laminated structures. Excessive loads or low velocity impact can cause matrix cracks and delaminations that may severely degrade the load carrying capability of the composite laminated structures. To develop the health monitoring techniques providing on-line diagnostics of smart composite structures can be helpful in keeping the composite structures sound during their service. In this presentation, we discuss the signal processing techniques and some applications for health monitoring of composite structures using piezoceramic sensors and fiber optic sensors.

Key words: *Health monitoring composite structures, Matrix cracks, Delaminations, Time-frequency analysis, Wavelet transform, Fiber optic sensor, Acoustic emission*

1. INTRODUCTION

The behavior of composite structures under impact or in-service loading has been the focus of health monitoring research - usage monitoring and damage monitoring - for sometime. Usage monitoring includes the measurement of strain and temperature during service of the composite structure. The precise characterization of impact damage in composites is an extremely difficult task in damage monitoring. This is partly because damage initiation and evolution in composite materials are highly complex phenomena involving various failure modes. Many recent studies have focused on the prediction of impact damages and the residual strength of composites. For structures susceptible to impact, routine nondestructive testing must be performed over the entire surface. A few examples of the traditional methods are X ray and ultrasonic method. Due to recent advances in sensor technology, a new concept of damage diagnostics for monitoring the integrity of in-service structures has been proposed [1,2].

The active sensing diagnosis (ASD) was proposed to detect the impact damage in in-service composite structures using piezoceramic sensors and actuators to generate and receive diagnostic waves by Chang [3]. In the previous research, the Fourier transform has been used successfully in extracting important features from signals for the passive sensing diagnosis (PSD) system [4,5]. The PSD system may be simpler and more lightweight than the ASD system with actuators. Recently, the PSD method using the time-frequency analysis has been issued. A method named wavelet transform (WT) can provide the time-frequency localization from sensor signals. The WT itself is a more intuitive decomposition of the data since it provides simultaneous time-frequency localization. Being a more flexible method of time-frequency decomposition, wavelets can describe signal characteristics in a much more precise manner and result in more accurate feature extraction.

The purpose of this paper is to describe and analyze the characteristics of the low-velocity impact damage in composite laminates and to monitor the health of composite structures under service loading using piezoceramic and fiber optic sensors. This paper proposes that the PSD method using the WT can be applied to monitor AE signals due to damage initiation of composite laminates during the low velocity impact.

2 . IMPACT DAMAGE MONITORING

2.1. Diagnostics of impact damages

The impact monitoring process provides diagnostics of composite structures susceptible to an impact load. This process is composed of two major functions; the impact identification and the diagnostics of impact damage. In other words, this concept of the impact monitoring combines the usage monitoring and the damage assessment techniques.

This paper proposed the PSD method that measures the characteristic frequency of AE signals. In the previous research, AE signals can be characterized by measuring the parameters such as counts, hit rates, energy, power spectrum, etc. These cannot properly distinguish the damage modes of composite laminates. The AE sensor system is too expensive to be applied to the real structural health monitoring system. In this paper, we used the PZT sensor to detect the frequency ranges characterized by the previous researches. This sensor was properly chosen to detect the propagating acoustic waves due to impacts and the AE due to initiation of damages of composites.

As a fundamental approach, the characteristics of the AE signals due to matrix cracks and the evolution of delamination are investigated. Tension tests were

Corresponding author:
Chun-Gon Kim, cgkim@kaist.ac.kr

performed to observe the time-frequency characteristics of the AE waves due to matrix cracks and free-edge delamination using $[\pm 45_2/0_2/90_2]_S$ Gr/Ep specimens. The differences of transient characteristics of the AE waves due to matrix cracks and delaminations can be identified by the time-frequency analysis. The WT can be used to characterize damage modes by measuring the transient decomposed signals of a certain scale level of wavelets.

2.2. Wavelet analysis

In order to overcome the limitations of harmonic analysis, it has been considered to use the alternative families of orthogonal basis functions called wavelets, instead of sines and cosines. The WT decomposes a signal into a set of basis functions that are localized in both time and frequency. Each wavelet function $\Psi_{a,b}(t)$ is a stretched or narrowed version of a prototype wavelet $\Psi(t)$, as shown in Fig. 1.

$$\Psi_{a,b}(t) = \frac{1}{\sqrt{a}}\Psi\left(\frac{t-b}{a}\right) \quad (1)$$

where $a \in R^+$ and $b \in R$ are scale and shift parameters, respectively.

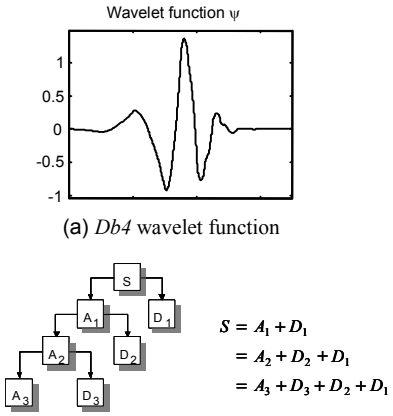

(a) *Db4* wavelet function

(b) Wavelet decomposition tree

Fig. 1. (a) *db4* wavelet function and (b) wavelet decomposition tree.

A function or a signal is expanded by a basis which is compactly supported in both time and frequency domains. For the actual computation of the WT, a and b should be discretized. This is called the Discrete Wavelet Transform (DWT). It turns out that analysis will be much more efficient if dyadic scales and positions, i.e. scales and positions are chosen based on powers of two, are employed. In the DWT, a signal may be represented by its approximations and details. An approximation is the high-scale, low frequency component of the signal. The details are the low-scale, high frequency components. The level of details j means the dyadic scales $a = 2^j$ $(j = 0,1,2\cdots,n)$. The approximation is calculated by the synthesis of other details over the level *j*. In this Fig. 1, 'S' represents the raw sensor signal, 'D_j' represent the details decomposed by the wavelets of scale a. 'A' represents the approximations. By selecting different dyadic scales, a signal can be broken into many lower-resolution components, referred as the wavelet decomposition tree.

3. DAMAGE MONITORING USING PIEZOCERAMIC SENSORS

3.1. Tension tests for matrix cracks and free-edge delaminations

Experiments are performed to investigate the characteristics of AE signals due to matrix cracks and delaminations. One strain gage and one PZT were used. The conventional AE sensor system has ability to detect AE signals up to 2 *MHz*. The AE signals of composite material have the characteristic frequency range of less than 500 *kHz*. Moreover, those of the delaminations are less than 250 *kHz*. The AE sensor system is too expensive in comparison with the cost of PZT sensor that is about $15. The PZT sensor was chosen to detect the AE signals having the frequency range from 20 *kHz* to 250 *kHz* known as the dominant frequency range due to damage such as matrix cracks and delaminations in composite laminates. The PZT made by Fuji Ceramics Co. has a circular disk shape of 2 *mm* in thickness and 5 *mm* in diameter.

The specimens are made of 16 plies of unidirectional graphite/epoxy prepreg with a stacking sequence of $[\pm 45_2/0_2/90_2]_S$. This laminate was chosen to produce free edge delaminations. CU-125NS prepreg tapes of HanKuk Fiber Co., Ltd. were used to make laminates. The material properties of CU125NS are E_1=130.0 GPa, E_2=E_3=10.0 GPa, G_{12}=G_{13}= 4.85 GPa, G_{23}=3.62 GPa, ν_{12}=ν_{13}=0.31, ν_{23}=0.52. In order to remove the flaws at the free edges due to the cutting process of the specimen, the free edges are treated successively by #220, 400, 800 and 1200 sandpaper. Tension tests was performed by INSTRON (model 4482) and loaded monotonically at the rate of 0.5 *mm/min*.

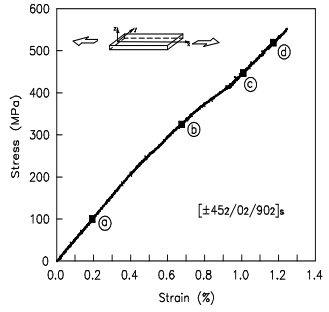

Fig. 2. Stress strain curve in tension test

Figure 2 shows the stress strain curve for tensile test. Figure 3 (a) shows the matrix cracks. In the side view of specimen, the out-of-plane deformation occurs considerably from the free edges due to the large delamination in the mid-plane as shown in Fig. 3 (b).

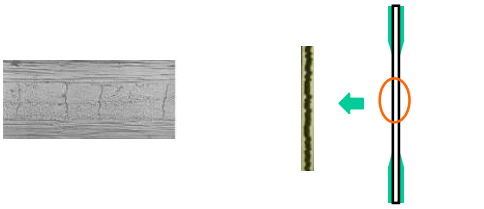

(a) Matrix cracks (b) Free-edge delamination

Fig. 3. Side view of specimen before ultimate failure and matrix cracks in $[\pm 45_2/0_2/90_2]_s$ laminate.

3.2. Low-velocity impact tests

The experiments for the diagnostics of AE signals due to impact damages were carried out to identify the distinguishing features of the AE waves in composite laminates. The complex damage signals were analyzed by the WT to investigate the characteristics of damages. We followed the previous experiments that studied the low-velocity impact phenomenon such as the damage mode and the mechanism of damage development [6]. The test equipment was the drop weight type impact machine as the same in this reference. The composite laminates had $[0_2/90_4]_S$ layups with the dimension of 140 *mm*×140 *mm*. The laminates were clamped along each edge with steel frames. One PZT sensor was attached on the laminates as shown in Fig. 4.

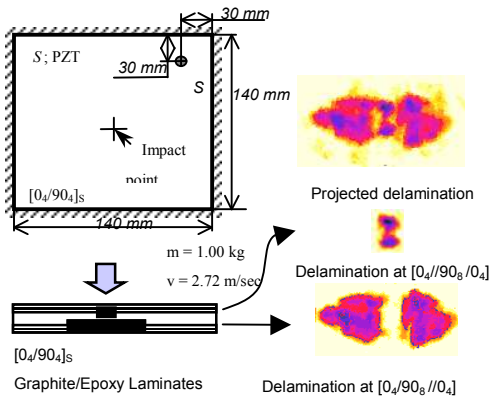

Fig. 4. Test specimen and the delaminations in 3.7 *J* impacted plate by C-Scan.

The sampling frequency was adjusted to 500 *kHz* in order to zoom in the frequency domain of signals. The acquired signal was processed by the anti-aliasing filter in the range of 20~250 *kHz*. From the results of the previous research, three levels of impact energy were chosen to generate no damage, hidden delaminations and a final fracture mode respectively. Firstly, the laminated plate was subjected to 0.1 *J* impact. After this impact, we confirmed that no damage was generated using the ultrasonic C-Scan. Secondly, after 3.7 *J* impact, delaminations having the dimension of 35 *mm*×20 *mm* were measured by the C-Scan, as shown in Fig. 4. Thirdly, after 6.0 *J* impact, it was observed that a final fracture mode with fiber breakage and delaminations.

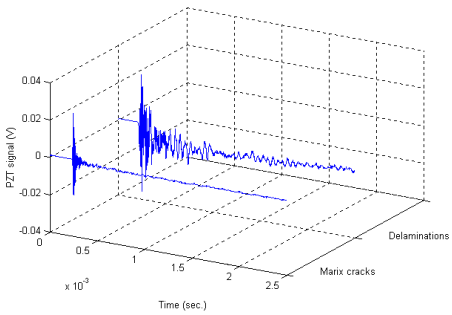

Fig. 5. PZT signals at the event of matrix cracks and free-edge delaminations.

3.3. Diagnostics of matrix cracks and free-edge delaminations

Figure 5 shows the acquired signals at the occurring time of matrix crack and the free-edge delaminations. The acquired signals were analyzed by the conventional spectral analysis and the WT to investigate the characteristics of AE signals for the comparison. During the tension test, matrix cracks were generated several times. The PZT signals due to matrix cracks have the similar pattern. The frequency spectrum of this signal is shown in Fig. 6 (a). The signals due to free-edge delaminations were obtained at the occurring time of out-of plane deformation from the load step (b) to (c) as shown in Fig. 2. The frequency spectrum of this signal is shown in Fig. 6 (b). It is obscure to classify the damage mode by the conventional Fourier Transform. These results only show the roughly different frequency ranges as the damage modes. The dominant frequency ranges of AE signals due to matrix cracks are above 350 *kHz* frequencies and those of the AE signals due to delaminations are below 250 *kHz*.

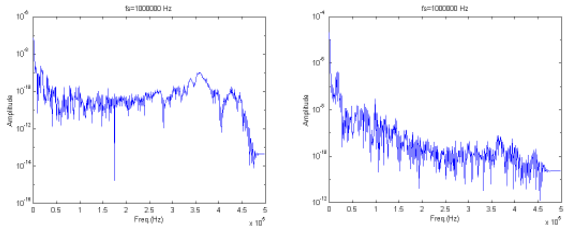

(a) matrix cracks (b) delaminations

Fig. 6. Frequency spectrums of PZT signals; (a) matrix cracks, (b) delaminations

Figure 7 shows the results of the WT decomposition of the acquired signal using the *db4* wavelet to the level 3 respectively. The *db4* stands for the 4th order Daubechies wavelet as shown in Fig. 1. The wavelet

functions have the advantage that they are localized with respect to both time and frequency and act as multiscale bandpass filters when convoluted with the signal data. The details are indicated by D_1^{1M} of which the subscript represents the level of decomposition and the superscript represents the sampling frequency. The details D_1^{1M}, D_2^{1M} and D_3^{1M} represent approximately 300~400 *kHz*, 140~240 *kHz*, 80~100 *kHz* signal range respectively from the calculation of approximate frequencies. Therefore, these details can represent the characteristic frequencies of AE signals. As the selection of wavelet functions, these details can show detailed characteristics that could not be represented by the harmonic function based analysis.

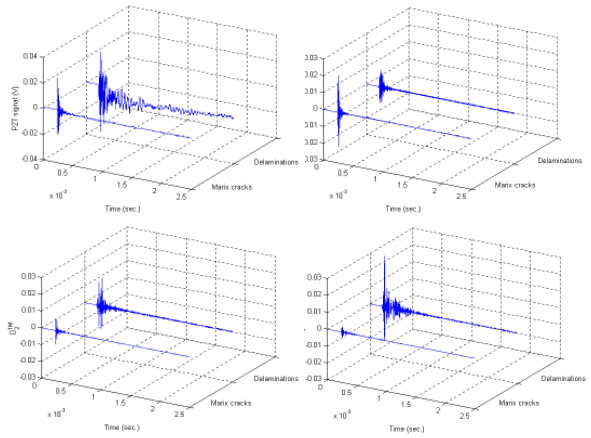

Fig. 7. Details D_1^{1M}~ D_3^{1M} of PZT signals of matrix cracks and delaminations by DWT.

Figure 7 shows that the AE signals due to matrix cracks are dominantly composed of the detail D_1^{1M}. However, the AE signals due to delaminations are mainly composed of D_2^{1M} and D_3^{1M}. These trends coincide with the frequency characteristics. From these results, delaminations known as the primary damage mode of low velocity impact can be detected by observing the details D_2^{1M} and D_3^{1M}. Therefore, the sampling frequency was adjusted to 500 *kHz* in order to zoom in the frequency domain of signals in the low-velocity impact test. Then, the details $D_1^{0.5M}$, $D_2^{0.5M}$ and $D_3^{0.5M}$ – the frequency ranges below about 250 *kHz* – represent the AE signals due to delaminations.

3.4. Diagnostics of impact damages

The frequency spectrums of these signals are shown in Fig. 8. These show that it is hard to distinguish the damage mode by the frequency spectrum.

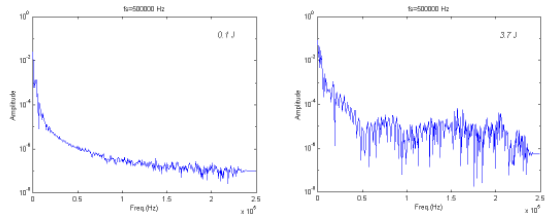

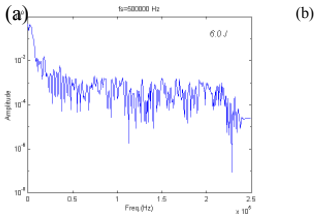

Fig. 8. Frequency spectrums of PZT signals of 0.1 *J*, 3.7 *J* and 6.0 *J* impacts

Figure 8(a) shows that AE signals were not detected during 0.1 *J* impact events. For 3.7 *J* impact, Fig. 8(b) shows that AE signals induced by the generation of delaminations can be observed by examining the frequency range of below 250 *kHz*. The characteristic frequencies were around about 40 *kHz*, and 130~200 *kHz*. For 6.0 *J* impact, Fig. 8(c) shows the higher amplitude of the signal due to severe damage, i.e., the final fracture mode. The time duration is shorter than that of 3.7 *J* impact, because the impact duration is shorter. The dominant frequencies were about 40 *kHz*, 80~100 *kHz,* and 150~200 *kHz*. It is not clear to identify the damage modes and the severity from the impact signal. The frequency spectrum only shows that the characteristic frequencies of AE signals have the wide band frequency and these dominant frequencies are slightly different by the damage modes.

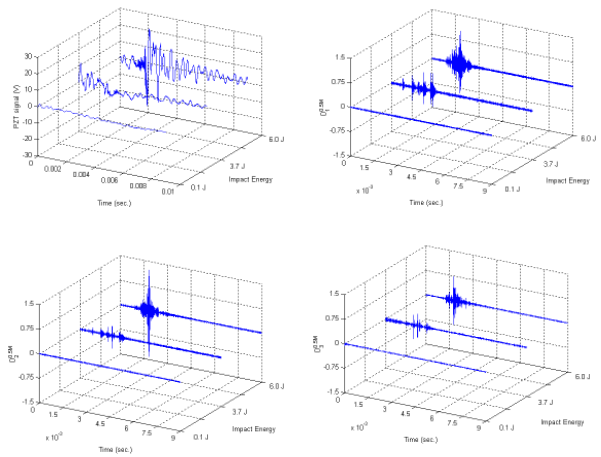

Fig. 9. Details $D_1^{0.5M}$~ $D_3^{0.5M}$ of PZT signals of 0.1 *J*, 3.7 *J* and 6.0 *J* impacts by DWT.

Figure 9 shows the results of the WT decomposition using the *db4* wavelet to the level 3 for three levels of impact energy respectively. From the previous results, the sampling frequency was adjusted to 500 *kHz* in order to zoom in the frequency domain of signals. Then, the details $D_1^{0.5M}$, $D_2^{0.5M}$ and $D_3^{0.5M}$ – the frequency ranges below about 250 *kHz* – represents the AE signals due to delaminations. For 0.1 *J* impact, there are very low detail signals. It indicates that the AE signals were not generated. For 3.7 *J* impact, the generation of

delamination can be estimated by the details. The details $D_1^{0.5M}$, $D_2^{0.5M}$ and $D_3^{0.5M}$ represent approximately 150~200 *kHz*, 70~120 *kHz*, 40~50 *kHz* signal respectively from the calculation of approximate frequencies. Therefore, these details represent the characteristic frequencies of AE signals. For 6.0 *J* impact, the higher amplitudes of $D_1^{0.5M} \sim D_3^{0.5M}$ were observed at the mode of final fracture with both delaminations and fiber breakage than those of the invisible delaminations. The details of this mode have about three times of amplitude than that of the delamination-dominant mode. The AE duration is shorter than that of the delamination-dominant mode. These make it possible to monitor the damage state by measuring the interesting detail components and adjusting the scale level.

4. DEPENDENCY OF MATRIX CRACKING SIGNAL UPON LAYUP SEQUENCE.

To characterize the matrix cracking, a kind of early stage fracture in composite layered structures, we analyzed the dependency of the matrix cracking signal upon layup geometry. Tensile test was done for crossply specimens to evaluate the matrix cracking characteristics using PZT as the AE sensor. Two types of layup geometry were selected in crossply laminated tensile specimens; 1) the 90-degree layers are varied with fixed 0 degree layer thickness, 2) 0/90 ratio is varied under fixed total laminate thickness. The specimen geometry is shown in Fig. 10. For the quantitative evaluation of matrix cracking signal dependency upon the layup geometry, the signal was processed using WT. In this experiment sampling rate was 1*MHz* and the details, $D_1^{1M} \sim D_4^{M}$ represent approximately 200~500 *kHz*, 100~300 *kHz*, 40~160 *kHz*, and 0~80 *kHz*, respectively.

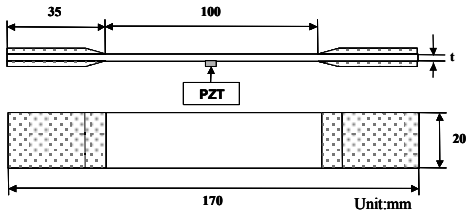

Fig. 10. Tensile test specimen for the matrix cracking signal acquisition.

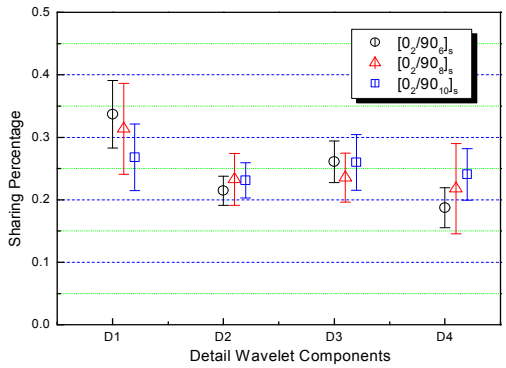

Fig. 11. Comparison of proportion of detail WT components. : $[0_2/90_6]_s$, $[0_2/90_8]_s$, $[0_2/90_{10}]_s$

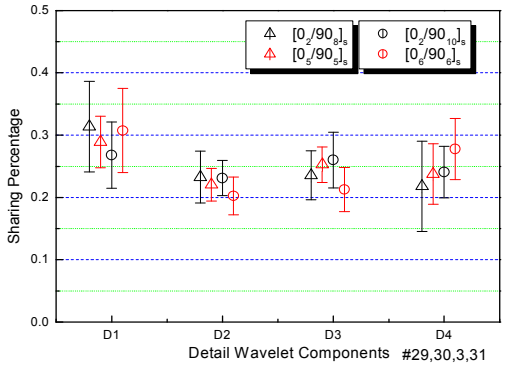

Fig. 12. Comparison of proportion of detail WT components. : $[0_2/90_8]_s$, $[0_5/90_5]_s$, $[0_2/90_{10}]_s$, $[0_6/90_6]_s$

Figure 11 shows the signal proportions of each detail component of matrix cracking signal for three layup geometries, $[0_2/90_6]_S$, $[0_2/90_8]_S$, $[0_2/90_{10}]_S$. As the total 90-layer thickness grows larger, the higher frequency detail D_1, has the smaller proportion while the lower frequency detail D_4 occupy the larger proportion in the matrix cracking signal. This trend can be similarly observed in send type of specimens in which the 0/90 ratio is varied with fixed total laminate thickness (Fig. 12).

5. HEALTH MONITORING OF COMPOSITES USING FOS

5.1. Simultaneous monitoring of smart composites

To perform the real-time health monitoring of the smart composite structures, two fiber optic sensor systems are proposed, which can measure the strain and detect the moment of fracture simultaneously. The two types of the coherent sources were used for the detection of fracture signals – EDFA (Erbium Doped Fiber Amplifier) with FBG and EDFA with Fabry-Perot filter. These sources were coupled to EFPI sensors embedded in composite specimens to monitor the fracture behavior of composites.

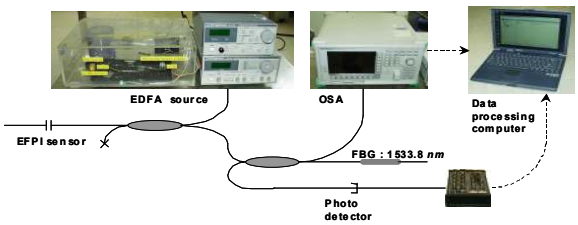

Fig. 13. Fiber optic sensor system for strain and fracture monitoring

In order to understand the characteristics of matrix cracking signals, we performed tensile tests using surface attached PZT sensors. This paper describes the implementation of time-frequency analysis such as short time Fourier-transform (STFT) for the quantitative evaluation of the fracture signals like matrix cracking.

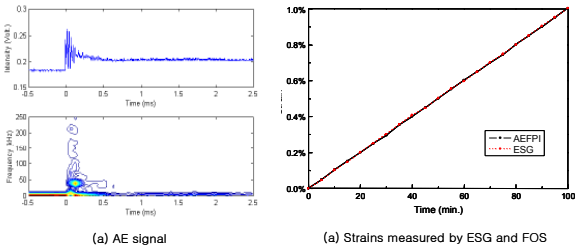

(a) AE signal (a) Strains measured by ESG and FOS

Fig. 14. AE fractural signal and strain measured by FOS

From the test of tensile load monitoring using fiber optic sensor systems, the measured strain agreed well with the value of electric strain gage and the fracture detection system could find out the moment of damage with high sensitivity to recognize the onset of micro-crack fracture signals.

5.2. Strain monitoring of smart wing box

Advanced composites are being extensively used for aerospace structures due to the high stiffness to weight and high strength to weight ratios. The stiffened wing boxes made of composite materials can be applied to aircraft fuselage or wing structure. As a practical application of aircraft structures, the composite wing box composed of two spars, four stiffeners, and two skins was fabricated [7]. Both the ends of the wing box were designed for clamping. Both the spars and the skins had the same stacking sequences of $[0_2/90/\pm45]_S$, and stiffeners had the stacking sequence of $[0_2/90/45/0/-45]_S$. The upper skin and two I-stiffeners were cured as one part. The lower skin and two I-stiffeners constituted the other part. These two co-cured stiffened skins were then secondary bonded by adhesive film with two spars. Total 24 FBG sensors were embedded in the composite wing box. FBG_A, FBG_B, and FBG_D lines were embedded in the upper skin, while, FBG_C line was embedded in the front spar. Figure 15 shows notation and location of the embedded FBG sensors. The selection of location of sensors was determined using the analytic results by the general-purpose finite element code, ABAQUS. The local buckling points of severe strain change were selected as the sensing points under bending load. A load cell was attached to the loading end. Electrical strain gages (ESG) were bonded on the surface of the wing box in order to compare the measured strain with that by FBG sensors. A LVDT (Linear Variable Differential Transformer) was used to measure vertical displacement.

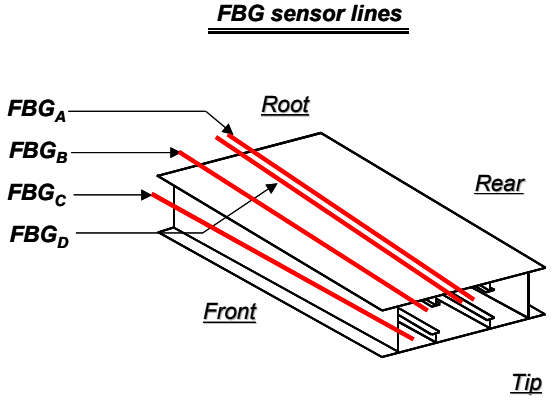

Fig. 15. Location and notation of FBG sensors

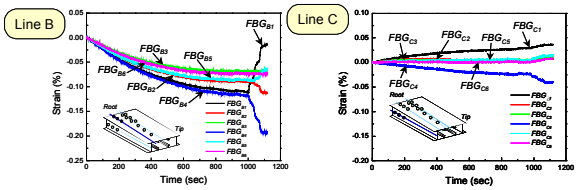

Fig. 16. Strains measured by FBG sensors – Line B and C

Strain vs. time curves by FBG sensors are shown in Fig. 16. In the sensor line B and C, pop-in (knee-point) phenomena were definitely observed at 920 seconds after the start of constant rate loading. These were caused by transient strain-release due to the failure of spar that plays a role of bearing the most of bending load. For the sensor lines A and D that were relatively far apart from the spar, strain-release effect from the spar was weakly propagated. The strains measured by FBG sensors were compared with strains by ESG and analytical results. At the previous strain vs. time curves, strain curves of FBG_B and FBG_C definitely branched into two paths. As a result, we were successfully able to measure the internal strains and determine the buckling point of the wing box using FBG sensors embedded in the wing box.

6. CONCLUSION

In this paper, we have presented the monitoring techniques for low-velocity impact damages of composite laminates using PZT and FOS. Also, included are some health monitoring applications using FOS.

For the fundamental approach, the characteristics of the AE signals due to matrix cracks and free-edge delaminations were investigated by the spectral analysis and the WT. From the spectral analysis, we have examined the characteristic frequencies of the AE signals. The spectral analysis exhibits low sensitivity to damage detection and poor diagnostic capability. The WT decomposes the signal into the several levels of detail.

From the results of wavelet analysis, the damage modes can be investigated by the details. The characteristic details of the AE signals due to matrix cracks and the evolution of free-edge delamination in the tension of $[\pm 45_2/0_2/90_2]_S$ Gr/Ep laminates under tensile load were analyzed. The AE signals due to matrix cracks are dominantly composed of the detail D_1^{1M} of *db4*. However, those due to delaminations are mainly composed of D_2^{1M} and D_3^{1M} of *db4*.

REFERENCES

1. Kudva, J.N., Marantidis, C. and Gentry, J.,"Smart Structures Concepts for Aircraft Structural Health Monitoring", *Proceedings of SPIE on Smart Structures and Materials*, 1993, Vol. 1917, p. 974-981.
2. Spillman Jr, W.B., Sirkis, J.S. and Gardiner, P.T., "Smart Materials and Structures; What are they?", *Smart Materials and Structures*, 1996; 5(3):247-254.
3. Chang, F.K., 1995. "Built-in Damage Diagnostics for Composite Structures", *Proceedings of ICCM-10*, V:283-289.
4. Sanders, G.W., and K. Chandrashekhara et al. 1997. "Fiber Optic Vibration Sensing and Neural Networks Methods for Prediction of Composite Beam Delamination", *Proceedings of SPIE on Smart Structures and Materials*, 3041:858-867.
5. Okafor, A.C., K. Chadrashekhara and Y.P. Jiang. 1996. "Delamination Prediction in Composite Beams with Built-in Piezoelectric Devices Using Modal Analysis and Neural Network", *Smart Materials and Structures*, 5(3):338-347.
6. Choi, I.H. and C.S. Hong. 1994. "Low-velocity Impact Response of Composite Laminates Considering Higher-order Shear Deformation and Large Deflection", *Mechanics of Composite Materials and Structures*, 1:157-170.
7. C. S. Hong, C. Y. Ryu, J. R. Lee, and C. G. Kim, “Buckling Behavior Monitoring of Composite Wing Box Model Using Fiber Bragg Grating Sensor System,” *Proc. Of SPIE 4327*, Newport Beach, California, USA, 2001.